BNL-60187R

Journal of Atmospheric Chemistry **20:** 259–280, 1995.

© 1995 *Kluwer Academic Publishers. Printed in the Netherlands.*

The Scavenging of Nitrate by Clouds and Precipitation

S. WURZLER[1], A. I. FLOSSMANN[2], H. R. PRUPPACHER[1] and S. E. SCHWARTZ[3]

[1]*Institute for Atmospheric Physics, Joh. Gutenberg University, D-6500 Mainz, Germany*
[2]*Université Blaise Pascal, Clermont-Ferrand, France*
[3]*Environmental Chemistry Division, Brookhaven National Laboratory, Upton, NY 11973, U.S.A.*

(Received: 17 January 1994; in final form: 20 June 1994)

Abstract. A model with spectral microphysics was developed to describe the scavenging of nitrate aerosol particles and HNO_3 gas. This model was incorporated into the dynamic framework of an entraining air parcel model with which we computed the uptake of nitrate by cloud drops whose size distribution changes with time because of condensation, collision-coalescence and break-up. Significant differences were found between the scavenging behavior of nitrate and our former results on the scavenging behavior of sulfate. These reflect the following chemical and microphysical differences between the two systems:

(1) nitrate particles occur in a larger size range than sulfate particles.
(2) HNO_3 has a much greater solubility than SO_2 and is taken up irreversibly inside the drops in contrast to SO_2.
(3) nitric acid in the cloud water is formed directly on uptake of HNO_3 gas whereas on uptake of SO_2 sulfuric acid is formed only after the reaction with oxidizing agents such as e.g., H_2O_2 or O_3.
(4) nitrate resulting from uptake of HNO_3 is confined mainly to small drops, whereas sulfate resulting from uptake of SO_2 is most concentrated in the largest, oldest drops, which have had the greatest time for reaction.

Sensitivity studies showed that the nitrate concentration of small drops is significantly affected by the mass accommodation coefficient.

Key words: Cloud physics, atmospheric chemistry, nitrate scavenging, air parcel model.

0. Definition of Symbols

a	drop radius
AP	aerosol particle (subscript)
avg	average (subscript)
d	drop (subscript)
$dlna$	logarithmic drop radius interval
D_a	Diffusion coefficient of gas in water (aqua) $\sim 10^{-5}$ cm^2 s^{-1}
D_g	diffusion coefficient of gas in air
D_v	diffusivity of water vapor in air
f	denotes a number (N) density distribution with f = dN/d ln(radius) in all graphs.

f_{APa}	aerosol particle number density distribution function for aerosol particles in air
f_{d}	cloud drop number density distribution function
F_{g}	ventilation coefficient for HNO_3
F_{v}	ventilation coefficient for water vapor in air $= 1.00 + 0.108X^2$ for $X \leq 1.4$, and $= 0.78 + 0.308X$, for $X > 1.4$, with $X = N_{\mathrm{Sc}}^{1/3} N_{\mathrm{Re}}^{1/2}$ (Pruppacher and Klett, 1978, p. 443)
g	denotes a mass (w) density distribution with $g = \mathrm{d}w/\mathrm{d}\ \ln(\text{radius})$ in all graphs.
g_{APa}	aerosol particle mass distribution function for aerosol in air
g_{APd}	aerosol particle mass density distribution for aerosol in cloud water
g_{Ga}	mass of HNO_3 in the air
$g_{\mathrm{Gd}}(m)$	mass density distribution function for dissolved HNO_3 in the drops
$g_{\mathrm{w}}(m)$	cloud drop mass distribution function = $m[1 - Q_{\mathrm{APd}}]f_{\mathrm{d}}(m)$
G	gas (subscript)
H	scale height
k_{mt}	mass transfer rate coefficient that incorporates interfacial and gas phase mass transport
K_{I}	dissociation coefficient for HNO_3 in water
K_{H}	Henry's Law coefficient for HNO_3 in water
K_{m}	turbulent eddy diffusion coefficient
K_{oa}	overall equilibrium coefficient for dissolution of HNO_3 in water $= K_{\mathrm{H}} \cdot K_{\mathrm{I}}$
L	liquid water content of the atmosphere in cm^3 of water per m^3 air
m	mass of drop
m_{a}	mass of air parcel
m_{AP}	mass of growing aerosol particle
n_i	aerosol particle number concentration of the ith log-normal distribution
N_{d}	total number of drops per unit volume
N_{APa}	total particle number concentration in the air
N_{Re}	Reynolds number $\approx V_\infty a/\nu_{\mathrm{a}}$
N_{Sc}	Schmidt number $= \nu_{\mathrm{a}}/D_{\mathrm{v}}$ for water vapor in air
$p_{\mathrm{HNO_3}}$	partial pressure of HNO_3
$p_{\mathrm{HNO_3,\,s}}$	partial pressure of HNO_3 at the drop surface
$p_{\mathrm{HNO_3,\,\infty}}$	partial pressure of HNO_3 at large distance from the drop
$Q_{\mathrm{APd}}(m)$	aerosol mass mixing ratio distribution function $= g_{\mathrm{APd}}(m)/(m f_{\mathrm{d}}(m))$
r	radius of growing aerosol particle
r_N	radius of dry aerosol particle
R	radius of the updraft
R_i	geometric mean radius of the ith log-normal distribution
R^*	universal gas constant cal. mol^{-1} K^{-1} in Equation (13) L atm. mol^{-1} K^{-1} in Equation (14)

S	drop surface (subscript)
T	absolute temperature
U	updraft velocity
$\mathbf{v}$	velocity field of air
v	mean molecular speed $=(8R^*T/\pi M)^{1/2}$ with R^* in erg mol^{-1} K^{-1} and molar mass in g mol^{-1}
V_∞	terminal velocity of drops
W	mass of liquid water or other substance per m^3
X	$=N_{\mathrm{Sc}}^{1/3}N_{\mathrm{Re}}^{1/2}$
z	vertical coordinate
α	mass accomodation coefficient
δ_{g}	gas film thickness $\approx a/F_{\mathrm{v}}$
ΔH°	standard enthalpy of reaction (298°K) describing temperature dependence of equilibrium constants $=17.3$ kcal/mol for dissolution of HNO_3 into water
μ	entrainment factor $=(1/m_{\mathrm{a}})(dm_{\mathrm{a}})/(dz)$ with m_{a} = mass of the air parcel
ν_{a}	kinematic viscosity of air
ψ	concentration of gases and aerosols inside the parcel
ψ'	concentration of gases and aerosols outside the parcel
Ψ	refers to the time rate change of the functions f_{d}, g_{APd}, g_{Gd}, f_{APa}, g_{APa}, Q_{APd}, m or m_{AP}
$\Psi\|_{\mathrm{act}}$	change due to activation of aerosol particles to drops
$\Psi\|_{\mathrm{AP,\,coll}}$	change due to aerosol particle collection
$\Psi\|_{\mathrm{cond,\,eva}}$	change due to condensation and evaporation
$\Psi\|_{\mathrm{d,\,coal}}$	change due to collision and coalescence of drops
$\Psi\|_{\mathrm{d,\,breakup}}$	change due to drop break-up
$\Psi\|_{\mathrm{d,\,uptake}}$	change due to uptake and desorption of gas
σ_i	standard deviation of the ith log-normal distribution
τ	characteristic time to establish equilibrium between gaseous and dissolved HNO_3
$\tau_{\mathrm{d.a.}}$	time constant characteristic of aqueous phase diffusion

1. Introduction

In recent years, the coastal seas of Europe have been plagued by an increased growth of algae causing serious pollution due to their decomposition. It is believed that the increased growth of algae is the result of an enhanced input of nitrogen compounds through the waters from rivers, which carry excess fertilizer compounds from agricultural activities. It is estimated that a similar amount of nitrogen enters the coastal seas via precipitation.

Nitrogen compounds enter clouds and precipitation through nitrate containing aerosol particles, such as $NaNO_3$ or NH_4NO_3, and through nitrogen containing gases, such as NO_2, NO, N_2O_5, HNO_2, HNO_3, NH_3 and PAN, most of which are due to anthropogenic sources. On entering cloudwater, these gases may be converted by a variety of reactions to ammonium, nitrite and nitrate compounds (see Schwartz, 1984; Seinfeld, 1986).

In the present study we are concerned with a marine atmosphere in which we assume that HNO_3 is taken up by cloud drops in the presence of $NaNO_3$, NaCl and $(NH_4)_2SO_4$. $NaNO_3$ is considered to have formed by reactions of HNO_3 with NaCl in sea salt particles (Kadowski, 1977). We realize that this scenario represents a gross-over simplification of the true marine atmosphere, as in the real world there certainly are other species affecting the uptake of HNO_3. We therefore consider this work merely a first attempt to bring out some of the main characteristic features of nitrogen scavenging. We also assume that during the lifetime of the model cloud which we study, the composition of the gas phase in the cloud environment does not change by gas phase reaction, so that we do not need to consider gas phase reactions within that time span. In addition, we assume that NO and NO_2 do not contribute to the nitrate content of the cloud water due to their relatively low solubility in water (Schwartz, 1984). We also postpone to a later study the contribution of N_2O_5 and HNO_2 to nitrogen scavenging, as these are mainly found in a night time atmosphere (Finlayson-Pitts and Pitts, 1986). We further neglect the possibility, that sea salt particles may be alkaline (Twohy *et al.*, 1989) and that HNO_3 may be taken up or desorbed by aerosol particles before activation. We plan to take these omitted factors into account in the model at some later stage. Such an incorporation would also need to take into account the surface properties of the particles involved and the reaction kinetics of high concentrated solutions, a problem on which there is still not enough information available.

Previously, we have studied the scavenging of gaseous and particulate sulfur compounds in the presence of H_2O_2 and O_3 by applying our cloud parcel model with entrainment (Flossmann *et al.*, 1985, 1987) and our two dimensional model for convective clouds (Flossmann and Pruppacher, 1988; Flossmann, 1991, 1993). There are several reasons to believe, that the scavenging of nitrogen compounds will proceed quite differently than the scavenging of sulfur compounds. Some of the reasons for this belief are:

(1) In contrast to $(NH_4)_2SO_4$ particles which are found mainly in the submicrometer size range, nitrate particles are observed to belong mostly to the supermicrometer particle size range, i.e. the same size range where NaCl particles are found (Fitzgerald, 1991).

(2) As shown in model calculations by Flossmann (1991), sulfate in cloudwater is present preferentially in drops belonging to the middle and smaller sizes of the drop size spectrum, whereas NaCl is present mainly in the water of cloud drops at the upper end of the drop spectrum. It is thus expected that $NaNO_3$ will also appear mainly in the drops of the upper end of the size spectrum.

(3) SO_2 is taken up by cloudwater as *S(IV)* and becomes subsequently converted to *S(VI)* mainly by intervention of suitable oxidizing agents, such as H_2O_2 and O_3. Thus, the production of acid from SO_2 takes some time, and consequently SO_2 is most concentrated in the largest, oldest drops, which have had the longest time for oxidation, whereas HNO_3 enters the cloud water directly as acid.

(4) The solubility of HNO_3 is much larger than that of SO_2. Thus HNO_3 is expected to appear readily as acid following the nucleation of cloud drops. The high solubility of HNO_3 also suggests that mass accommodation would affect the nitrate concentration of the cloud drops, an effect not observed during the uptake of SO_2.

(5) These facts suggest that one would expect considerable differences between nitrate and sulfate with respect to the rate at which nitrate will appear in the cloud water of a growing cloud, the rate at which the pH of the cloud water will be affected, and the rate at which the scavenged species will be redistributed inside the cloud drop spectrum during its evolution in time.

In the present paper we report on computations we have made with our cloud parcel model to investigate with detailed microphysics the extent to which the expected differences in the scavenging behavior of nitrate or sulfate are indeed found. In a second paper, to follow later, we shall include the detailed scavenging formulations used here in our 2-D dynamic model for convective clouds in order to study for actual observed scenarios the deposition of nitrogen species on the North Sea. Although cloud parcel models include the dynamic features of a convective cloud only in a very rough manner, they are useful to answer specific questions on microphysical processes in clouds. We also acknowledge the fact that in real clouds air is not isotropically and homogeneously entrained into the cloud and that the air from the environment is not continuously and instantaneously mixed into the cloud independently of locations around the cloud, as it is assumed in our cloud parcel model. However, present inhomogeneous mixing models include dynamic realism at the expense of a variety of other processes (see Roesner *et al.*, 1990). We therefore proceeded to apply our isotropic entrainment model to the problem at hand.

2. The Present Model

The basic dynamic framework employed in the present study is the entraining air parcel model discussed in detail by Flossmann *et al.* (1985). The formulations for the cloud microphysic processes and for aerosol particle scavenging are also given in Flossmann *et al.* (1985). A scavenging model for two or more types of aerosol particles simultaneously present in air has been given by Flossmann (1991). A model which describes the uptake of gases by cloud drops has been formulated by Flossmann *et al.* (1987) and Flossmann (1993).

Following our earlier studies, the present model treats the cloud microphysical and scavenging processes in a spectral form and assumes the presence of one pollutant gas and three aerosol particle types to be present in the air parcel whose size distributions change with time due to entrainment, activation to drops and impaction on drops. The size distribution of the corresponding cloud drops changes in time due to condensation, evaporation, collision and coalescence, and break up. The concentration of the gaseous species in the parcel is assumed to change in concentration with time by mass transport to and into the drops and by entrainment of outside air. The model follows the aerosol particle mass and gas mass inside each drop size category in time as materials are scavenged and re-distributed inside the changing drop size spectrum.

Here we briefly summarize the main features of the model; the above cited references should be consulted for details. The present model calculates the time rate of change of the density distribution functions for the aerosol particles in the air $\psi_{\mathrm{APa}}(m_{\mathrm{AP}})$ as

$$\begin{aligned}\frac{\partial \psi_{\mathrm{APa}}(m_{\mathrm{AP}})}{\partial t} &= -\nabla \cdot [\mathbf{v}\psi_{\mathrm{APa}}(m_{\mathrm{AP}})] + \nabla \cdot [K_m \nabla \psi_{\mathrm{APa}}(m_{\mathrm{AP}})] + \\ &+ \left.\frac{\partial \psi_{\mathrm{APa}}(m_{\mathrm{AP}})}{\partial t}\right|_{\mathrm{act}} + \left.\frac{\partial \psi_{\mathrm{APa}}(m_{\mathrm{AP}})}{\partial t}\right|_{\mathrm{con/eva}} + \\ &+ \left.\frac{\partial \psi_{\mathrm{APa}}(m_{\mathrm{AP}})}{\partial t}\right|_{\mathrm{AP,\,coll}},\end{aligned} \tag{1}$$

where $\psi_{\mathrm{APa}}(m_{\mathrm{AP}})$ represents the aerosol particle number density distribution function $f_{\mathrm{APa},\,(\mathrm{NH_4})_2\mathrm{SO_4}}(m_{\mathrm{AP}})$, $f_{\mathrm{APa,\,NaCl}}(m_{\mathrm{AP}})$ and $f_{\mathrm{APa,\,NaNO_3}}(m_{\mathrm{AP}})$ for $(NH_4)_2SO_4$, NaCl and $NaNO_3$ particles in the air, respectively, and the mass density distribution function $g_{\mathrm{APa},\,(\mathrm{NH_4})_2\mathrm{SO_4}}(m_{\mathrm{AP}})$, $g_{\mathrm{APa,\,NaCl}}(m_{\mathrm{AP}})$ and $g_{\mathrm{APa,\,NaNO_3}}(m_{\mathrm{AP}})$ for $(NH_4)_2SO_4$, NaCl and $NaNO_3$ particles in the air, respectively: The time rate of change of the gas phase concentration g_{Ga} of the HNO_3 mass in the air can be written as

$$\frac{\partial g_{\mathrm{Ga}}}{\partial t} = -\nabla \cdot [\mathbf{v} g_{\mathrm{Ga}}] + \nabla \cdot [K_{\mathrm{m}} \nabla g_{\mathrm{Ga}}] - \int_0^\infty \left.\frac{\partial g_{\mathrm{Ga}}(m)}{\partial t}\right|_{\mathrm{uptake}} dm \tag{2}$$

with $\mathbf{v}$ = velocity field of air and K_{m} = eddy mixing coefficient.

The time rate of change of the density distribution functions for the drops $\psi_{\mathrm{d}}(m)$ is

$$\begin{aligned}\frac{\partial \psi_{\mathrm{d}}(m)}{\partial t} &= -\nabla \cdot [\mathbf{v}\psi_{\mathrm{d}}(m)] + \nabla \cdot [K_{\mathrm{m}} \nabla \psi_{\mathrm{d}}(m)] + \frac{\partial}{\partial z}[V_\infty \psi_{\mathrm{d}}(m)] + \\ &+ \left.\frac{\partial \psi_{\mathrm{d}}(m)}{\partial t}\right|_{\mathrm{act}} + \left.\frac{\partial \psi_{\mathrm{d}}(m)}{\partial t}\right|_{\mathrm{con,\,eva}} + \left.\frac{\partial \psi_{\mathrm{d}}(m)}{\partial t}\right|_{\mathrm{AP,\,coll}} + \\ &+ \left.\frac{\partial \psi_{\mathrm{d}}(m)}{\partial t}\right|_{\mathrm{d,\,coal}} + \left.\frac{\partial \psi_{\mathrm{d}}(m)}{\partial t}\right|_{\mathrm{d,\,break}} + \left.\frac{\partial \psi_{\mathrm{d}}(m)}{\partial t}\right|_{\mathrm{d,\,uptake}}\end{aligned} \tag{3}$$

where $\psi_d(m)$ is the cloud drop number density distribution function $f_d(m)$, the mass density distribution function $g_{APd,\,(NH_4)_2SO_4}(m_{AP})$, $g_{APd,\,NaCl}(m_{AP})$ and $g_{APd,\,NaNO_3}(m_{AP})$ for particulate $(NH_4)_2SO_4$, NaCl and $NaNO_3$ dissolved in the drops, respectively, and the mass density distribution function $g_{Gd,\,HNO_3}(m)$ for HNO_3 gas dissolved in the drops, respectively, with m = mass of drop, m_{AP} = mass of aerosol particle, $\Psi = \partial\psi_d(m)/\partial t$ = time rate change of the functions f_d, g_{APd}, g_{Gd}, f_{APa}, g_{APa}. $\Psi|_{act}$ = change due to activation of aerosol particles to drops (nucleation scavenging), $\Psi|_{con/eva}$ = change due to condensation and/or evaporation of drops, $\Psi|_{AP,\,coll}$ = change due to aerosol particle collection (impaction scavenging), $\Psi|_{d,\,coal}$ = change due to collision and coalescence of drops, $\Psi|_{d,\,break}$ = change due to drop breakup, $\Psi|_{d,\,uptake}$ = change due to uptake of gases in drops (only calculated for g_{Gd}). Herein, f denotes a number density distribution function and g a mass distribution function. AP stands for aerosol particle, G for gas, a for air and d for drop.

In order to adapt Equations (1), (2) and (3) to an entraining air parcel model the first two terms in Equations (1), (2) and the first three terms in Equation (3) are replaced by the terms $-\mu[\psi_{APa}(m_{AP}) - \psi_{APa}(m_{AP})']U$ for the aerosol particles, $-\mu[g_{Ga} - g'_{Ga}]U$ for the gas and $\mu\psi_d(m)U$ for the drops. Those terms describe the entrainment. The entrainment of air, HNO_3 gas and aerosol particles (size dependent), and the detrainment of drops are treated with the entrainment factor $\mu = 0.6R$. Here R is the radius of the updraft. Note that the primed quantities refer to the parcel's environment and U represents the updraft velocity. The amount of gas in the environment is allowed to decrease in proportion to the density of the air. The amount of aerosol particles in the environment is allowed to decrease with height at differing rates depending on size.

The nucleation scavenging and condensational growth of the aerosol particles considered and their scavenging by drops are described by the relations given in Flossmann *et al.* (1985) and Flossmann (1991). However, the uptake of HNO_3 by the formed drop has to be considered in some greater detail. HNO_3 undergoes the following reactions with liquid water (Schwartz and White, 1981):

$$HNO_3(g) + H_2O(l) \rightleftharpoons HNO_3(aq), \tag{4}$$

$$HNO_3(aq) \rightleftharpoons H^+ + NO_3^-. \tag{5}$$

The equilibrium relations for these two reactions are

$$K_H = \frac{[HNO_3]_{aq}}{p_{HNO_3}}, \tag{6}$$

$$K_1 = \frac{[H^+][NO_3^-]}{[HNO_3]_{aq}}. \tag{7}$$

K_H is the Henry's law coefficient and K_1 the dissociation coefficient for HNO_3. The overall reaction may be written as:

$$HNO_3(g) + H_2O(l) \rightleftharpoons H^+ + NO_3^-, \tag{8}$$

with the overall equilibrium coefficient K_{oa}:

$$K_{oa} = K_H \cdot K_1 = \frac{[H^+][NO_3^-]}{p_{HNO_3}} \tag{9}$$

At equilibrium the total N(V) concentration is given by

$$\begin{aligned}[N(V)] &= [NO_3^-] + [HNO_3]_{aq} \\ &= [NO_3^-]\left(1 + \frac{[HNO_3]_{aq}}{[NO_3^-]}\right) \\ &= [NO_3^-]\left(1 + \frac{[H^+]}{K_1}\right).\end{aligned} \tag{10}$$

Eliminating $[NO_3^-]$ by combining Equations (9) and (10) we find

$$p_{HNO_3} = \frac{[H^+][N(v)]}{K_{oa}\left(1 + \frac{[H^+]}{K_1}\right)}. \tag{11}$$

The equilibrium constant K_1 is not well established but has a value of approximately 15.1 M at 298 K. In view of this since in cloud water $[H^+] \ll 15$ M, then to good approximation $([H^+]/K_1) \ll 1$, so that at equilibrium

$$p_{HNO_3} = \frac{[H^+][N(V)]}{K_{oa}}, \tag{12}$$

where K_{oa} is given by Schwartz and White (1981) as

$$K_{oa} = 3.3 \times 10^6 \exp\left[-\frac{\Delta H}{R^*}\left(\frac{1}{T} - \frac{1}{298}\right)\right] \tag{13}$$

with K_{oa} in mol^2 liter^{-2} atm^{-1}, $\Delta H = -17.3$ kcal mol^{-1}. Here R^* is the universal gas constant and T is the temperature in K.

The mass transport of nitric acid from the gas phase to the solution droplets, treated as reversible process is described by

$$\frac{d[N(V)]}{dt} = \frac{k_{mt}}{R^*T} \cdot F_g \cdot (p_{HNO_3,\infty} - p_{HNO_3,S}) \tag{14}$$

where k_{mt} is the mass transfer rate coefficient that incorporates interfacial and gasphase mass transport, $p_{HNO_3,\infty}$ is the partial pressure of nitric acid in the bulk gas phase of the cloud, $p_{HNO_3,S}$ is the nitric acid partial pressure in equilibrium with the aqueous phase concentration of $[H^+]$ and $[NO_3^-]$, and F_g is the ventilation coefficient for HNO_3.

The total concentration of N(V) species in a drop is given by the sum of N(V) derived from $HNO_3(g)$ and $NaNO_3$(AP):

$$[N(V)]_{tot} = [N(V)_G + [N(V)]_{AP} \tag{15}$$

and, hence, to good approximation

$$p_{\mathrm{HNO_3},\,S} = \frac{[\mathrm{H}^+]([\mathrm{N}(V)]_\mathrm{G} + [\mathrm{N}(V)]_\mathrm{AP})}{K_\mathrm{oa}}\,, \tag{16}$$

where the concentrations refer to the average in the drop.

The large value for K_oa implies that the equilibrium partial pressure is much less than the initial ($p_{\mathrm{HNO_3},\,S} \ll p_{\mathrm{HNO_3},\,\infty}$). Thus for example for $[\mathrm{H}^+] = 10^{-3}$ M and $[\mathrm{N}(V)] = 10^{-2}$ M, $p_{\mathrm{HNO_3},\,S} = 3 \times 10^{-12}$ atm, which in our particular case, where the initial partial pressure of HNO_3 ranges between 4.5×10^{-10} atm and 1×10^{-9} atm, is well below the initial partial pressure of the gas.

We therefore may assume that the uptake of HNO_3 can be treated essentially as an irreversible process due to its high solubility. This result was verified by a sensitivity study in which we deliberately set $p_{\mathrm{HNO_3},\,S} = 0$ in Equation (14). As expected, the uptake of $\mathrm{N}(V)$ thus computed differed only negligibly from the uptake computed from Equation (14) together with Equation (16).

The mass transfer rate coefficient k_mt in Equation (14) is given by

$$k_\mathrm{mt} = \left(\frac{a^2}{3D_\mathrm{g}} + \frac{4a}{3v\alpha}\right)^{-1} \tag{17}$$

where a is the drop radius, D_g the gas-phase diffusion coefficient, v the mean molecular speed and α the mass accommodation coefficient.

We next consider the ventilation coefficient $F_\mathrm{g} = F_{\mathrm{HNO_3}}$ in Equation (14). Unfortunately $F_{\mathrm{HNO_3}}$ is not known. However, Baboolal *et al.* (1981) computed ventilation coefficients for gases with Schmidt numbers between 0.1 and 5.0 from a numerical solution of the complete convective diffusion equation and found only a very small effect of the Schmidt numbers on the ventilation coefficient. Since $F_{\mathrm{HNO_3}}$ as well as $F_\mathrm{v} = 0.71$ lie within this range of Schmidt numbers we set $F_{\mathrm{HNO_3}} = F_\mathrm{v} = 1.00 + 0.108\,X^2$ for $X \leq 1.4$, and $= 0.78 + 0.308\,X$, for $X > 1.4$, with $X = N_\mathrm{Sc}^{1/3} N_\mathrm{Re}^{1/2}$ (Pruppacher and Klett, 1978, p. 443).

Because of the large solubility of HNO_3, the equilibrium between gaseous and dissolved HNO_3 is not established within the model time step of 2 sec. An estimated characteristic time for establishing equilibrium of a highly soluble gas (Levine and Schwartz, 1982; Jacob, 1985; Schwartz, 1986) is

$$\tau \approx \left[\int k_\mathrm{mt}\left(\frac{4\pi}{3}a^3\right)\left(\frac{\mathrm{d}N}{\mathrm{d}a}\right)\mathrm{d}a\right]^{-1}, \tag{18}$$

where the integral is taken over the drop size distribution of the cloud. For a monodisperse cloud having drop radius $a = 5\,\mu$m, a liquid water content $L = 0.5 \times 10^{-6}$ cm^3 water per m^3 air, $\alpha = 0.07$ (Van Doren *et al.*, 1990), $v = 3.2 \times 10^4$ cm s^{-1} and D_g ranging between 0.15 cm^2 s^{-1} (268 °K) and 0.193 cm^2 s^{-1} (293 °K), the characteristic time τ is about 15 sec. This time is much greater than the internal mixing time of the drop $\tau_\mathrm{d.a.} = (a^2)/(\pi^2 D_\mathrm{a})$ (Schwartz, 1986) which for $a = 5\,\mu$m

is about 2×10^{-3} s. Hence the drop can be considered to be well mixed so that to a good approximation $[H^+]_s = [H^+]_{avg.}$ and $[N(V)]_s = [N(V)]_{avg.}$. The assumption also seems justified in view of the experiments of Mitra *et al.* (1990) for the uptake of SO_2 at atmospheric gas concentrations.

The ions in the cloud water of our model are subject to the following condition of electroneutrality:

$$[Na^+]_{NaNO_3} + [H^+] = [NO_3^-]_G + [NO_3^-]_{AP}. \tag{19}$$

Actually we should have added for completeness $[Na^+]_{NaCl}$ and $2[NH_4^+]$ on the left-hand side and $[Cl^-]$ and $[SO_4^{2-}]$ on the right hand side due to the presence of $(NH_4)_2SO_4$ and NaCl in the cloud water. However, neither of these salts contributes to $[H^+]$ nor to $[NO_3^-]$ so we may neglect them in the ion balance. Considering $[Na^+]_{NaNO_3} = [N(V)]_{AP}$ and writing $[NO_3^-]_G = [N(V)]_G$ and $[NO_3^-]_{AP}$ we find after substituting Equation (7) into Equation (19) and arranging the terms

$$[H^+]^2 + (K_1 + [N(V)]_{AP})[H^+] - K_1[N(V)]_G = 0 \tag{20}$$

from which $[H^+]$ and therefore pH = –log $[H^+]$ may be computed from known values of $[N(V)]_{AP}$ and $[N(V)]_G$. Equation (20) may be simplified since $[H^+] \ll K_1$ so that $[H^+]$ may be computed with sufficient accuracy from

$$[H^+] = \frac{K_1[N(V)]_G}{K_1 + [N(V)]_{AP}} \approx [N(V)]_G. \tag{21}$$

This result was verified by another sensitivity study in which we solved Equation (20) with and without the quadratic term. Furthermore, tests showed that $[H^+]$ always remained below 0.003 M so that the formation of HSO_4^- in the solution could be disregarded.

3. Cases Chosen for Evaluation

As in Flossmann *et al.* (1985) the temperature and humidity distribution assumed for the present study were those used by Lee *et al.* (1980). The initial updraft radius of the air parcel was assumed to be 350 m and the initial updraft speed was assumed to be 1 m s^{-1}.

For the marine aerosol particle size distribution we chose the distribution observed by Hoppel *et al.* (1990) during a ship cruise in the tropical atlantic ocean far from anthropogenic sources (see their Figures 7 and 8 curve 4). We fitted this spectrum by superimposing three log-normal distributions

$$\begin{aligned} \frac{dN_{APa}}{d\ln r_N} &= f_{APa}(\ln r_N) \\ &= \sum_{i=1}^{3} f_{APa,i}(\ln r_N) \\ &= \sum_{i=1}^{3} \frac{n_i}{(2\pi)^{1/2}\log\sigma_i \ln 10} \exp\left(-\frac{[\log(r_N/R_i)]^2}{2(\log\sigma_i)^2}\right), \end{aligned} \tag{22}$$

TABLE I. Parameters for the marine aerosol particle distribution as given in Equation (22); n_i = number of aerosol particles per cm^3, R_i = geometric mean aerosol particle radius in μm, σ_i = standard deviation in mode i

Mode i	n_i	R_i	$\log \sigma_i$
1	100	0.027	0.25
2	120	0.105	0.112
3	12	0.12	0.45

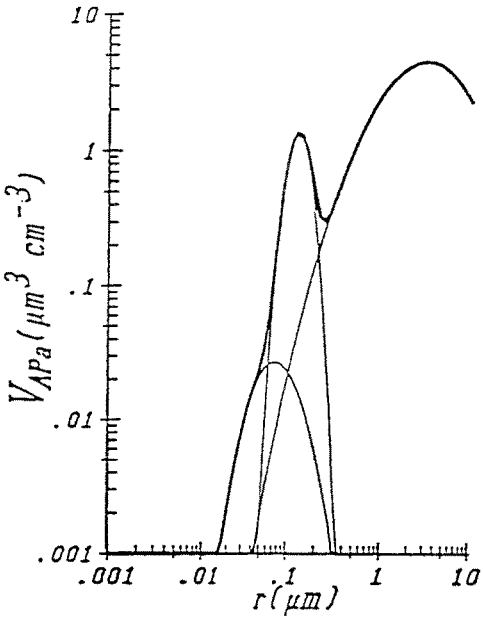

Fig. 1. Volume density distribution for aerosol particles of maritime type resulting from Equation (22) and Table I; total number concentration $N_{\mathrm{APa}} = 222.5$ cm^{-3}, and total particle mass $w_{\mathrm{APa}} = 22$ μg m^{-3} (in the aerosol particle size range between 0.97×10^{-3} μm and 10.08 μm).

where r_N is the radius of the 'dry' aerosol particles, R_i is the geometric mean radius, n_i is the aerosol particle number concentration and σ_i is the standard deviation of the ith log-normal distribution. N_{APa} is the total particle number concentration in air. The parameters n_i, R_i and σ_i for this aerosol spectrum have the values given in Table I, resulting in the volume distribution as given in Figure 1.

In Figure 1 the two modes in the submicrometer size range were assumed to be due to aerosol particles consisting of $(NH_4)_2SO_4$ while the third mode, covering mainly the size range above 1 μm, was assumed to consist of particles derived initially from sea salt each internally mixed of NaCl and $NaNO_3$ in proportions between 10% and 25% $NaNO_3$ ranging from 2 to 5 μg m^{-3}. The mixing ratio of

TABLE II. Listing of the initial conditions for cases 1 to 3

Case	HNO_3 (ppb(v))	Mass of HNO_3 ($\mu g\ m^{-3}$)	% of $NaNO_3$	Mass of $NaNO_3$ ($\mu g\ m^{-3}$)	$\frac{[N(V)]_{gas}}{[N(V)]_t}$ (%)
1	0.45	1.27	10	2.02	44.96
2	1	2.72	10	2.02	64.31
3	0.45	1.27	25	5.05	24.64

TABLE III. Listing of observed particulate nitrate and HNO_3 concentrations in the air

(a) Particles

Observer	Range of nitrate concentration in air ($\mu g\ m^{-3}$)	Conditions
Savoie *et al.* (1987)	0.16	background air
Parungo *et al.* (1987)	0.1–0.2	background air
Huebert and Lazrus (1980a)	0.13–0.25	background air
Berresheim *et al.* (1990)	0.25	background air
Kadowaki (1977)	1.2–5.7	moderately polluted areas
Wolff *et al.* (1986)	1.58	moderately polluted areas
Erisman *et al.* (1988)	10.5	moderately polluted areas

(b) HNO_3

Observer	Range of HNO_3 in air (ppb(v))	Conditions
Huebert and Lazrus (1980b)	0.08–0.11	remote areas
LeBel *et al.* (1990)	0.03–0.29	remote areas
Leaitch *et al.* (1991)	0.46–6.4	moderately polluted areas
Wolff *et al.* (1986)	0.7	moderately polluted areas
Erisman *et al.* (1988)	4.3	moderately polluted areas

HNO_3 in the air was assumed to vary between 0.45 ppb(v) and 1ppb(v) (1ppb(v) = 1nmol/mol(air)). The various scenarios used are summarized in Table II. In case 1 there is about as much aerosol nitrate as gaseous nitrate available for scavenging. For case 2 the gaseous nitrate available for input dominates, while for case 3 the particulate nitrate dominates. The parameters chosen for our computations and listed in Table II are representative of the field observations listed in Table III.

The concentration of the aerosol particles in the two modes covering the submicrometer size range (Figure 1) was assumed to have a scale height of 5 km, while the concentration of the particles in the third mode covering mainly the size range

above 1 μm was assumed to have a scale height of 3 km. HNO_3 was assumed to decrease with height as the total air pressure. A further sensitivity study showed that our results and conclusions were not substantially affected by the various differences in vertical concentration profiles.

For the mass transfer coefficient k_{mt} that incorporates interfacial and gas-phase mass transport we chose a mass accommodation coefficient α of 0.1 (Ponche *et al.*, 1993). Although the mass accommodation coefficient for the uptake of HNO_3 gas in *clean water* is known (Van Doren *et al.*, 1990; Ponche *et al.*, 1993) we do not have enough information yet about a mass accommodation coefficient for polluted droplets like they are typically present in clouds. Therefore we decided to carry out our sensitivity studies for α ranging between 0.1 and 1.

4. Results

The results of our model computations for case 1 are given in Figures 2 and 3 for the model times 200 and 1600 sec. The results for case 2 and case 3 are given in Figure 4 for a model time of 1600 sec.

If two curves are displayed in the same figure, the dashed lines represent the results of the sensitivity studies with a mass accommodation coefficient $\alpha = 0.1$ and the solid lines represent the model results for a mass accommodation coefficient $\alpha = 1.0$. If only the solid line is visible, it is valid for both cases $\alpha = 0.1$ and $\alpha = 1.0$.

From Figures 2a and 3a we notice that the liquid water mass, which after 200 sec is still confined to the small drop size end of the spectrum, has after 1600 sec model time shifted to encompass the precipitation size drops. Comparing the Figures 2a and 3a with 2b and 3b, we notice that the main mass of scavenged HNO_3 follows the main water mass. The same result has been found for the uptake of SO_2 by Flossmann *et al.* (1987, 1994). As expected from our previous results for $(NH_4)_2SO_4$ particles (Flossmann *et al.*, 1985, 1987; Flossmann, 1991), the main mass of scavenged $NaNO_3$ mass follows closely the main water mass in the drop size spectrum (not shown here). The re-distribution of scavenged gas and aerosol mass is a consequence of the collision and coalescence process. In Figures 2b and 3b no appreciable effect of the mass accommodation coefficient on the nitrate mass in the drops is obtained. In Figures 2c and 3c we have displayed the variation with drop size of the mixing ratio of aerosol mass in the cloud water per kg of air. We notice that below a drop radius of 10 μm, Q_{APd} increases strongly with decreasing drop size as a consequence of continuous entrainment and activation of fresh aerosol particles. The small secondary maximum near 20 μm drop radius corresponds to the initial activation of aerosol particles at the cloud base. Comparison with Figure 2a shows that the secondary maximum is associated with very little water mass (see, e.g., Ogren and Charlson, 1992). A consequence of this is reflected in Figure 2d where we notice that the concentration of nitrate in this size range assumes a maximum. On the other hand we find in Figure 2d no maximum in the

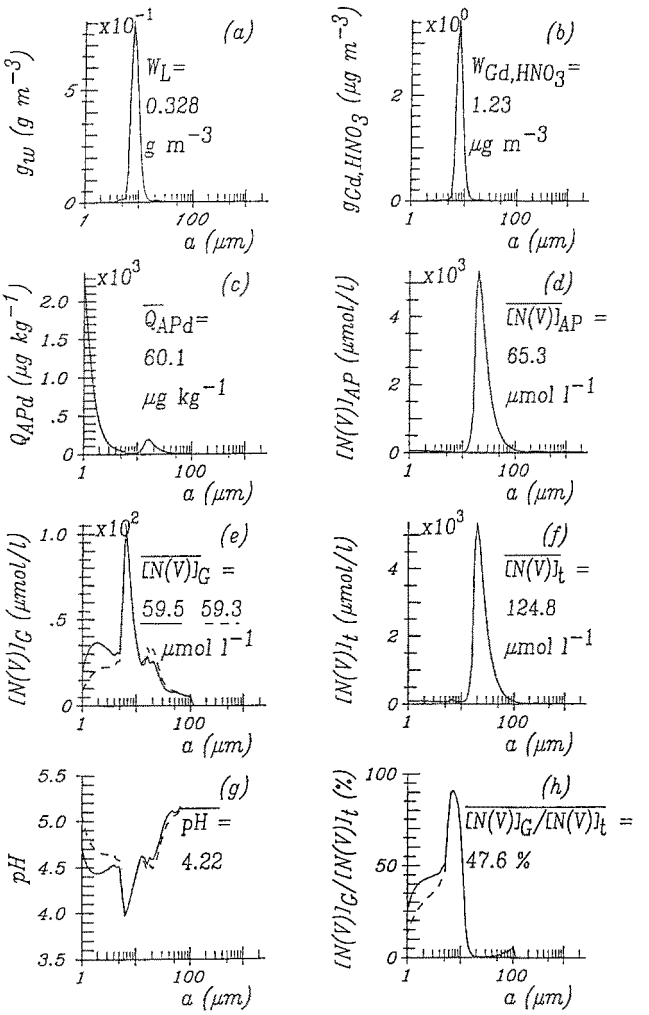

Fig. 2. Results of case 1 for a model time of $t = 200$ sec. (a) Water mass density distribution function g_w (w_l is the liquid water content), (b) nitric acid mass density distribution function $g_{Gd,\,HNO_3}$ in the drops from gas scavenging ($w_{Gd,\,HNO_3}$ is the total nitric acid mass), (c) concentration of scavenged aerosol particle mass in the drops ($\overline{Q_{APd}}$ is the average aerosol particle concentration in the water), (d) concentration of nitrate in the drops from aerosol particle scavenging ($\overline{[N(V)]_{AP}}$ is the average nitrate concentration), (e) concentration of nitrate in the drops from gas scavenging ($\overline{[N(V)]_G}$ is the average nitrate concentration with the value 59.5 μmol per liter for $\alpha = 1.0$ and the value 59.3 μmol per liter for $\alpha = 0.1$), (f) total concentration of scavenged nitrate in the drops ($\overline{[N(V)]_t}$ is the average total nitrate concentration), (g) pH in the drops ($\overline{pH}$ is the average pH derived from the average concentration of H^+ ions), (h) gaseous nitrate with respect to the total nitrate in the drops ($\overline{[N(V)]_G/[N(V)]_t}$ is the average fraction). The density distribution functions are displayed per logarithmic radius interval d ln a.

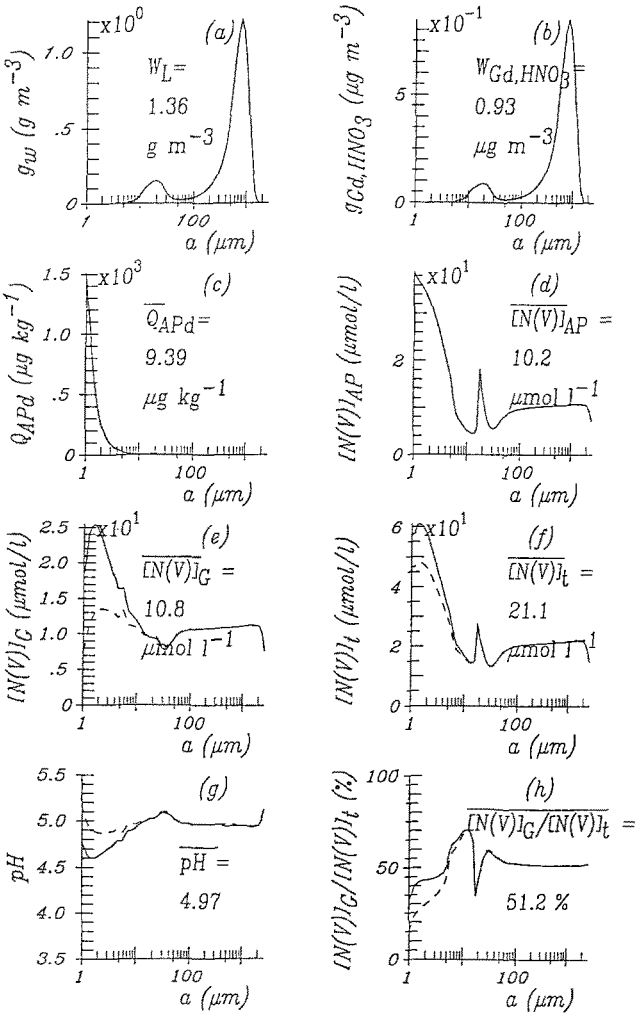

Fig. 3. Results of case 1 for a model time of $t = 1600$ sec. The density distribution functions are displayed per logarithmic radius interval d ln a.

nitrate concentration at the very small drop size end of the spectrum as expected from Figure 2c. This of course is a result of the fact that the strong increase in Q_{APd} for $a \leq 10$ μm is due to $(NH_4)_2SO_4$ particles, which we assumed to encompass the lower two modes in the assumed aerosol particle size distribution. Thus, these particles will not show up in Figure 2d, where we have plotted the nitrate content of the cloud water contributed by dissolved aerosol particles. After 1600 sec model time the secondary maximum of the nitrate concentration in the cloud water near $\alpha \approx 20$ μm still persists. In addition, however, a nitrate maximum also appears in the cloud water for $a \leq 10$ μm. As expected, it is caused by the entrainment of $NaNO_3$ particles whose contribution to the nitrate content of the cloud water increases with increasing model time. In Figure 2e the concentration of (N[V)] in

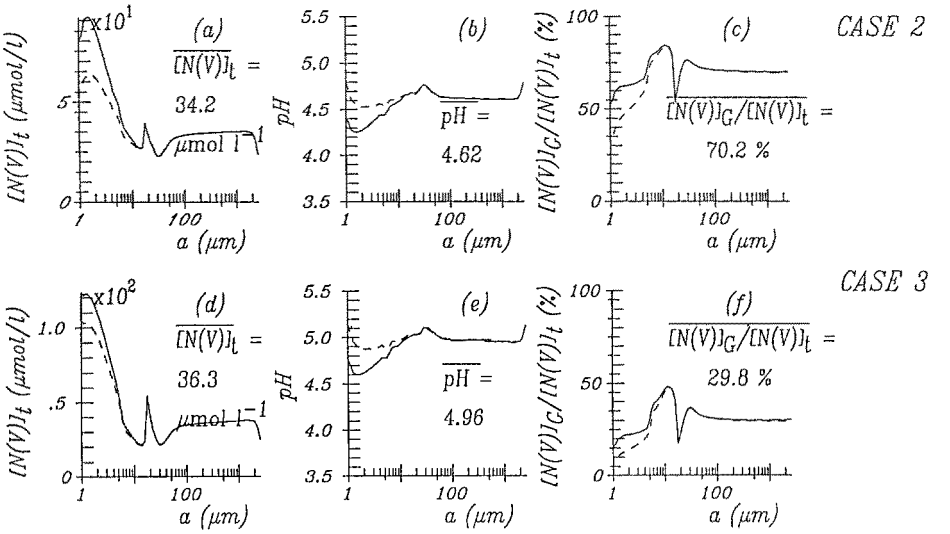

Fig. 4. Results of cases 2 and 3 for a model time of $t = 1600$ sec. (a) Case 2: total concentration of scavenged nitrate in the drops ($\overline{[N(V)]_t}$ is the average total nitrate concentration), (b) Case 2: pH in the drops ($\overline{pH}$ is the average pH derived from the average concentration of H^+ ions), (c) Case 2: gaseous nitrate with respect to the total nitrate in the drops ($\overline{[N(V)]_G/[N(V)]_t}$ is the average fraction). (d) Case 3: total concentration of scavenged nitrate in the drops ($\overline{[N(V)]_t}$ is the average total nitrate concentration), (e) Case 3: pH in the drops ($\overline{pH}$ is the average pH derived from the average concentration of H^+ ions), (f) Case 3: gaseous nitrate with respect to the total nitrate in thedrops ($\overline{[N(V)_G/[N(V)]_t}$ is the average fraction). The density distribution functions are displayed per logarithmic radius interval d ln a.

cloud water due to the uptake of HNO_3 is displayed. We notice the pronounced concentration maximum inside drops near 7 μm radius. This is a result of the high solubility of HNO_3 which readily enters the first cloud drops as soon as they have formed. This process rapidly depletes the gaseous HNO_3, so that at the initial stages of condensation ($t = 200$ sec.) the subsequently nucleated drops have less HNO_3 available for scavenging. The HNO_3 concentration in drops larger than 7 μm decreases with increasing size due to the radius dependency of the gas uptake.

The nitrate concentration in drops with radius $a \leq 6$ μm is seen to be quite sensitive to a variation of the mass accommodation coefficient (see Figure 2e). Our model calculations with a mass accommodation coefficient α of 0.1 give a 40% lower average nitrate concentration in drops smaller than 6 μm than calculations with a mass accommodation coefficient α of 1.0. As for the model calculations with $\alpha = 0.1$ the small drops take up less HNO_3, so that the larger drops have slightly more gas available for scavenging than in calculations with a mass accommodation coefficient α of 1.0. Since the uptake of HNO_3 and its dissociation in water determines the pH in the cloud water, we expect and indeed find in Figure 2g the lowest value in pH in the drop size range where the maximum of the HNO_3 concentration

occurs in Figure 2e. With decreasing HNO_3 concentration in the cloud water the pH rises again. As expected from its effect on the nitrate concentration the mass accommodation coefficient also affects the pH. Figure 2g shows that for $\alpha = 0.1$ the pH of the small drops is higher than for $\alpha = 1.0$. Figures 2e and 2g show that almost all HNO_3 has dissociated.

Figures 3e and 3g show that at a model time of 1600 sec larger drops are present and that these drops have received HNO_3 both via collision and coalescence with smaller drops as well as by uptake of entrained HNO_3 gas on their own. Although the efficiency of HNO_3 scavenging is radius dependent, the concentration of all drops with $a \geq 50$ μm appear to have a rather uniform nitrate concentration. This is the result of the collision and coalescence process which allows the smaller drops with higher concentration to coalesce with larger drops of lower concentration. At the model time 1600 sec the average nitrate concentration in drops of radii smaller than 20 μm is now about 30% lower for an α of 0.1 than for an α of 1.0.

In Figures 2f and 3f we have plotted the total concentration of [N(V)] in the cloud water i.e. the sum of the gaseous and particulate contribution. Figures 2h and 3h give the ratio of the nitrate concentration due to the uptake of HNO_3 gas to the total nitrate concentration in the cloud water. We notice from Figure 2h that for $a \leq 5$ μm and for $a > 12$ μm nitrate from $NaNO_3$ dominates the total nitrate concentration in the cloud water. On the other hand, the contribution from HNO_3 dominates in the size range 5 to 12 μm. Since at $t = 200$ sec the main liquid water content is also found in this size range (see Figure 2a), the contribution of NO_3^- from HNO_3 to the total NO_3^- is as much as 47.6%; this corresponds roughly to the initial supply ratio of nitrate (see Table II). As expected from Figure 3e this ratio increases to 51.2% (see Figure 3h) after $t = 1600$ sec. because of the increased concentration of NO_3^- from HNO_3 in the range of $a \geq 50$ μm.

For cases 2 and 3 we have plotted in Figure 4 the concentration of nitrate and pH in the cloud water as well as the relative contribution of the nitrate from HNO_3 uptake to the total nitrate inside the drops. The spectral behavior of the other parameters behave similar to those discussed in Figures 2 and 3. We notice from Figure 4c that the relative contribution of the HNO_3-derived nitrate in the cloud water has increased now to 70.2%, as expected from the fraction of HNO_3 available in the air (see Table II). As expected, the relative contribution of the HNO_3 derived nitrate decreases to 29.8% if the initial fraction in the air has also decreased by about the same ratio (see Figure 4f and Table II).

From cases 1 to 3 we find that the total nitrate concentration in the cloud water decreases from a range of 125–225 μmol/l at 200 sec to a range of 21–36 μmol/l at 1600 sec. This reduction by one order of magnitude results from the fact that the liquid water content of the cloud increased during this time by a factor of 4 while the nitrate increased through scavenging of freshly entrained material only by about 30%, e.g. from 0.93 to 1.23 μg/m^3 in case 1.

In general, we notice that the calculated nitrate mass in the cloud water lies within the values observed in relatively clean air masses as Isaac *et al.* (1990)

reported between 0.56 and 12.75 $\mu g/m^3$, Leaitch *et al.* (1991) observed 0.07–1.24 $\mu g/m^3$, and Leaitch *et al.* (1992) reported an average of 0.14 $\mu g/m^3$ for a cumulus cloud. The same is true for the total concentration of nitrate and the pH. Those, however, can only be compared with observations in precipitation water. There, Galloway *et al.* (1982) observed between 0.3–50.5 μmol/l (pH = 4.9), Galloway *et al.* (1988) reported an average of 3–4.5 μmol/l (pH = 4.96–4.97), Church *et al.* (1988) measured 3–16 μmol/l (pH = 5.1–4.38), Galloway *et al.* (1983) 5.5–27.3 μmol/l (pH = 4.8–4.2), and Schaug *et al.* (1987) reported 50–64 μmol/l over the North Sea with an average pH between 4.3–4.5.

5. Summary and Conclusions

We have developed a spectral microphysical model to simulate the drop size dependent scavenging of nitrate aerosol particles and HNO_3 gas. We have coupled this model to the simple dynamics of an entraining air parcel model. With the combined models we have simulated the scavenging of nitrate by cloud drops whose size changes in time as a consequence of condensation, collision-coalescence and break-up for a typical loading of marine air with particulate and gaseous nitrate.

In general, the obtained aqueous phase nitrate concentrations and pH values are consistent with those found in moderately polluted areas around the globe. Specifically, our model results allow the following conclusions:

(1) During the evolution in time of a drop size spectrum, collision and coalescence re-distribute inside the cloud water the nitrate scavenged from HNO_3 gas and $NaNO_3$ aerosol particles. This redistribution takes place in such a way that the main nitrate mass is always associated with the main water mass in the cloud, i.e., the main nitrate mass is contained in the larger drops which may reach the ground as precipitation. This result is analogous to that found by us earlier for the scavenging of SO_2 gas and $(NH_4)_2SO_4$ particles.

(2) Close to the cloud base ($t = 200$ sec.) the nitrate concentration due to scavenging of nitrate particles has its maximum in drops between 10 and 100 μm radius, with almost no nitrate in drop smaller than 10 μm. Only in the later stages ($t = 1600$ sec.) nitrate also appears in the small drops of $a < 10$ μm due to the activation of entrained nitrate particles.

This behavior is due to the fact that in marine air nitrate is generally found in the size range above 1 μm radius, where also NaCl particles are found. Some of these particles become chemically converted to $NaNO_3$ by reaction of NaCl with HNO_3 (Kadowski, 1977). In contrast, nucleation scavenging of $(NH_4)_2SO_4$ particles result in a sulfate mixing ratio, which increases for drops with $a \leq 10$ μm with decreasing drop size (Flossmann, 1985) because sulfate particles are contained mainly in the size range lower than 1 μm (Fitzgerald, 1991).

(3) The nitrate resulting from the uptake of HNO_3 is confined mainly to the small drops. This is a result of the high solubility of HNO_3, which causes that it

becomes readily dissolved in the cloud drops as soon as they are nucleated. This result is in contrast to the uptake of SO_2 which oxidizes to sulfate only in the presence of oxidizing agents such as O_3 and H_2O_2 (Flossmann *et al.*, 1987). Sulfate formed in this manner exhibits highest concentrations in the cloud water encompassing the large drop size end of the spectrum. This behavior is a result of the fact, that the largest drops are also the 'oldest' drops which have experienced oxidation of SO_2 to sulfate for the longest time.

(4) Scavenging of HNO_3 results in a pH of the cloud water which is lowest in the drops at the small size end of the spectrum. With increasing drop size the pH rises. This again is the result of the high solubility of HNO_3 and the behavior discussed in Section 3. This also contrasts the behavior of the pH resulting from the oxidation of SO_2 in the cloud water. Since the oxidation process requires time to form acid so that the lowest pH due to SO_2 oxidation is found in the largest drops (Flossmann *et al.*, 1987).

(5) Nucleation scavenging of nitrate particles and gas scavenging of HNO_3 are both very efficient mechanisms which act immediately at cloud formation. Consequently, the fraction of gaseous versus particulate nitrate found in the cloud water is determined almost exclusively by their supply in the air and does not change significantly during cloud evolution unless an air mass with different nitrate fraction would be advected. This result is in contrast to nucleation scavenging of sulfate particles and gas scavenging of SO_2 where the latter is taken up by clouds only slowly and in relation to oxidizing agents present.

(6) Variations in the mass accommodation coefficient appear to affect significantly the nitrate concentration due to the uptake of HNO_3 by drops less than 20 μm, but have no noticeable effect on the total mass of scavenged HNO_3 gas. Thus for drops with a radius smaller than 20 μm the nitrate concentration for $\alpha = 0.1$ was 30 to 40% lower than for α 1. This means that the mass accommodation coefficient has a significant effect on those cloud drops which are remaining in the cloud after the precipitation has fallen out and the cloud is forced to evaporate leaving behind new aerosol particles by drop to particle conversion. In contrast the nitrate content of drops which are large enough to fall out as rain was found to be independent of α in the range 0.1 to 1.0.

(7) In contrast to the scavenging of SO_2 the uptake of HNO_3 under atmospheric conditions seems to be an almost irreversible process due to its high solubility.

Acknowledgements

This research was funded by the CEC under contract no. STEP-CT90-0047. The authors also acknowledges with gratitude the financial support of the Ministry for Research and Technology of the Federal Republic of Germany under project 325-4007-07EU7148 and of the Deutsche Forschungsgemeinschaft under project Fl 186/1-1 and the Sonderforschungsbereich 233.

Part of this research has been carried out during a visit of one of us (S.W.) at the Brookhaven National Laboratory whose support is hereby thankfully acknowledged. The work at Brookhaven National Laboratory was conducted under Contract No. DE-AC02-76CH00016 with the U.S. Department of Energy. The authors of this paper are solely responsible for its content.

References

Baboolal, L. B., Pruppacher, H. R., and Topalian, J. H., 1981, A sensitivity study of a theoretical model of SO_2 scavenging by water drops in air, *J. Atmos. Sci.* **38**, 856–870.

Berresheim, H., Andreae, M. O., Ayers, G. P., Gillett, R. W., Merrill, J. T., Davis, V. J., and Chameides, W. L., 1990, Airborne measurements of dimethylsulfide, sulfur dioxide, and aerosols ions over the southern ocean south of Australia, *J. Atmos. Chem.* **10**, 341–370.

Church, T. M., Galloway, J. N., Jickells, T. D., and Knap, A. H., 1982, The chemistry of western atlantic precipitation at the mid-atlantic coast and on Bermuda, *J. Geophys. Res.* **87**, 11013–11018.

Durham, J. L., Barnes, H. M., Overton, J. H., 1984, Acidification of rain by oxidation of dissolved sulfur dioxide and absorption of nitric acid, in J. L. Durham (ed.), *Chemistry of Particles, Fog and Rain*, Butterworth, London.

Erisman, J. W., Vermetten; A. W. M., Asman, W. A. H., Waijers-IJpelaan, and Slanina, J., 1988, Vertical distribution of gases and aerosols: The behaviour of ammonia and related compounds in the lower atmosphere, *Atmos. Environ.* **22**, 1153–1160.

Fitzgerald, J. W., 1991, Marine aerosols: A review, *Atmos. Environ.* **25A**, 533–545.

Finlayson-Pitts, B. J. and Pitts, J. N., 1986, *Atmospheric Chemistry*, Wiley, New York.

Flossmann, A. I., 1994, A 2-D spectral model simulation of the scavenging of gaseous and particulate sulfate by a warm marine cloud, *J. Atmos. Res.* **32**, 233–248.

Flossmann, A. I., 1991, The scavenging of two different types of marine aerosol particles calculated using a two-dimensional detailed cloud model, *Tellus* **43B**, 301–321.

Flossmann, A. I., Hall, W. D., and Pruppacher, H. R., 1985, A theoretical study of the wet removal of atmospheric pollutants. Part I, *J. Atmos. Sci.* **42**, 582–606.

Flossmann, A. I., Pruppacher, H. R., and Topalian, J. H., 1987, A theoretical study of the wet removal of atmospheric pollutants. Part II, *J. Atmos. Sci.* **44**, 2912–2923.

Flossmann, A. I. and Pruppacher, H. R., 1988, A theoretical study of the wet removal of atmospheric pollutants. Part III, *J. Atmos. Sci.* **45**, 1857–1871.

Galloway, J. N., Likens, G. E., Keene, W. C., and Miller, J. M., 1982, The composition of precipitation in remote areas of the world, *J. Geophys. Res.* **87**, 8771–8786.

Galloway, J. N., Knap, A. H., and Church, T. M., 1983, The composition of western atlantic precipitation using shipboard collectors, *J. Geophys. Res.* **88**, 10859–10864.

Galloway, J. N., Tokos, J. T., Knap, A. Y., and Keene, W. C., 1988, Local influences on the composition of precipitation on Bermuda, *Tellus* **40B**, 178–188.

Hoppel, W. A., Fitzgerald, J. W., Frick, G. M., Larson, R. E., and Mack, E. J., 1990, Aerosol size distributions and optical properties found in the marine boundary layer over the atlantic ocean, *J. Geophys. Res.* **95**, 3659–3686.

Huebert, B. J. and Lazrus, A. L., 1980a, Tropospheric gas phase and particulate nitrate measurements, *J. Geophys. Res.* **85**, 7322–7328.

Huebert, B. J. and Lazrus, A. L., 1980b, Bulk composition of aerosols in the remote troposphere, *J. Geophys. Res.* **85**, 7337–7344.

Isaac, G. A., Leaitch, W. R., and Strapp, J. W., 1990, The vertical distribution of aerosols and acid related compounds in air and cloudwater, *Atmos. Environ.* **24a**, 3033–3046.

Jacob, D. J., 1985, Comment on 'The photochemistry of a remote stratiform cloud' by William L. Chameides, *J. Geophys. Res.* **90**, 5864.

Kadowaki, S., 1977, Size distribution and chemical composition of atmospheric particulate nitrate in the Nagoya area, *Atmos. Environ.* **11**, 671–675.

Leaitch, W. R., Isaac, G. A., Strapp, J. W., Anlauf, K. G., Wiebe, H. A., MacPherson, J. I., 1988, Chemical and microphysical case studies of towering cumuli in Ontario, 1988. *Preprint Volume of the 7th Joint Conf. on Applications of Air Pollution Meteorology with AWMA. Jan. 1991, New Orleans*, 232–237.

Leaitch, W. R., Isaac, G. A., Strapp, J. W., Banic, C. M., and Wiebe, H. A., 1992, The relationship between cloud droplet number concentrations and anthropogenic pollution: Observations and climatic implications, *J. Geophys. Res.* **97**, 2463–2474.

LeBel, P. J., Huebert, B. J., Schiff, H. I., Vay, S. A., Van Bramer, S. E., and Hastie, D. R., 1990, Measurements of tropospheric nitric acid over the western United States and northeastern Pacific Ocean, *J. Geophs. Res.* **95**, 10199–10204.

Lee, I. Y., Hänel, G., and Pruppacher, H. R., 1980, A numerical determination of the evolution of cloud drop spectra due to condensation on natural aerosol particles, *J. Atmos. Sci.* **37**, 1839–1853.

Levine, Z. S. and Schwartz, S. E., 1982, In-cloud and below-cloud scavenging of nitric acid and acid vapor, *Atmos. Environ.* **16**, 1725–1734.

Mitra, S. K. and Hannemann, A. U., 1993, On the scavenging of SO_2 by large and small rain drops: V. A wind tunnel and theoretical study of the desorption of SO_2 from water drops containing S(IV), *J. Atmos. Chem.* **16**, 201–218.

Ogren, J. A. and Charlson, R. J., 1992, Implications for models and measurements of chemical inhomogeneities among cloud droplets, *Tellus* **44b**, 208–225.

Parungo, F. P., Nagamoto, C. T., Madel, R., Rosinski, J., and Haagenson, P. L., 1987, Marine aerosols in Pacific upwelling regions, *J. Atmos. Sci.* **18**, 277–290.

Ponche, J. L., George, Ch., and Mirabel, Ph., 1993, Mass transfer at the air/water interface: Mass accommodation coefficients of SO_2, HNO_3 and NH_3, *J. Atmos. Chem.* **16**, 1–21.

Roesner, S., Flossmann, A. I., and Pruppacher, H. R., 1990, The effect on the evaluation of the drop spectrum in clouds on the preconditioning of air by successive convective elements, *QJRMS* **116**, 1389–1403.

Schaug, J., Hanssen, J. E., Nodop, K., Ottar, B., and Pacyna, J. M., 1987, Cooperative programme for monitoring and evaluation of the long range transmission of air pollutants in Europe (EMEP), summary report from the Chemical Coordinating Centre for the third phase of EMEP. EMEP-CCC-Report 3/87 (May 1987), Norwegian Institute for Air Research, Postboks 64, N-2001 Lillestrom, Norway.

Savoie, D. L., Prospero, J. M., and Nees, R. T., 1987, Nitrate, non-seasalt sulfate, and mineral aerosol over the northwestern Indian Ocean, *J. Geophys. Res.* **92**, 933–942.

Schwartz, S. E., 1984, Gas and aqueous phase chemistry of HO_2 in liquid-water clouds, *J. Geophys. Res.* **89**, 11589–11598.

Schwartz, S. E., 1986, Mass transport considerations pertinent to aqueous-phase reactions in liquid-water clouds, in W. Jeaschke (ed.), *Chemistry of Multiphase Atmospheric Systems*, Springer, Berlin, pp. 416–471.

Schwartz, S. E., 1984, Gas-aqueous reactions of sulfur and nitrogen oxides in liquid-water clouds, in J. G. Calvert (ed.), *SO_2, NO and NO_2 Oxidation Mechanisms*, Butterworth, Boston, pp. 173–208.

Schwartz, S. E. and White, W. H., 1981, Solubility equilibria of the nitrogen oxides and oxyacids in dilute aqueous solutions, in J. R. Pfafflin and E. N. Ziegler (eds.), *Advances in Environmental Science and Engineering, Vol. 4*, Gordon and Breach, New York, pp. 1–45.

Seinfeld, J. H., 1986, *Atmospheric Chemistry and Physics of Air Pollution*, Wiley, New York, 738 pp.

Twohy, C. H., Austin, P. H., and Charlson, R. J., 1989, Chemical consequences of the initial diffusional growth of cloud droplets: A clean marine case, *Tellus* **41B**, 51–60.

Van Doren, J. M., Watson, L. R., Davidovits, P., Worsnop, D. R., Zahniser, M. S., and Kolb, C. Z., 1990, Temperature dependency of the uptake coefficients of HNO_3, HCl and N_2O_5 by water droplets, *J. Phys. Chem.* **94**, 3265–3269.

Waltrop, A., Mitra, S. K., Flossmann, A. I., and Pruppacher, H. R., 1991, On the scavenging of SO_2 by cloud and rain drops: IV. A wind tunnel and theoretical study of the absorption of SO_2 in the ppb(v) range by water drops in the presence of H_2O_2, *J. Atmos. Chem.* **12**, 1–17.

Wolff, G. T., Ruthkosky, M. S., Stroup, D. P., Korsog, P. E., Ferman, M. A., Wendel, G. J., and Stedman, D. H., 1986, Measurements of SO_x, NO_x and aerosol species on Bermuda, *Atmos. Environ.* **20**, 1229–1239.